Journal of Crystal Growth 310 (2008) 5241–5247

Contents lists available at ScienceDirect

Journal of Crystal Growth

journal homepage: www.elsevier.com/locate/jcrysgro

Growth of mm-thick orientation-patterned GaAs for IR and THZ generation

C. Lynch [a,*], D.F. Bliss [a], T. Zens [a], A. Lin [b], J.S. Harris [b], P.S. Kuo [c], M.M. Fejer [c]

[a] Air Force Research Laboratory, Hanscom AFB, MA 01731, USA
[b] Solid State Photonics Laboratory, Stanford University, Stanford, CA 94305, USA
[c] E. L. Ginzton Laboratory, Stanford University, Stanford, CA 94305, USA

ARTICLE INFO

Article history:
Received 14 February 2008
Received in revised form
20 June 2008
Accepted 19 August 2008
Communicated by D.W. Shaw
Available online 30 August 2008

Keywords:
A3. Hydride vapor phase epitaxy
B1. Gallium arsenide
B2. Nonlinear optic materials

ABSTRACT

Low-pressure hydride vapor phase epitaxy (HVPE) is being used for the regrowth of thick GaAs on orientation-patterned templates for nonlinear optical frequency conversion. We have achieved epitaxial growth rates of 200 μm/h and produced millimeter-thick films in 10-h-long growth runs. A critical problem in the HVPE regrowth of orientation-patterned GaAs is the preservation of the original patterned structure—during thick growth, the domain walls often bend and annihilate. Measurements indicated that the domain wall bending decreased as the growth temperature was reduced. The substrate miscut and the orientation of unpatterned regions also affect the vertical propagation of domain walls. In this paper we discuss the process improvements which have facilitated the production of millimeter-thick layers with nearly vertical domain walls.

Published by Elsevier B.V.

1. Introduction

Infrared (IR) and terahertz (THz) frequency generation is of interest for use in spectroscopy, infrared countermeasures (IRCM) for aircraft protection, and THz imaging. Sources that are compact, efficient, and tunable, and which operate at room temperature are desirable. Frequency conversion in nonlinear optical (NLO) materials is one way to meet these specifications, especially when the NLO material is engineered to allow quasi-phasematching (QPM) [1]. In a QPM structure, a periodic inversion of the crystal orientation is used to induce a periodic reversal of the sign of the NLO coefficient. One of the most mature NLO material systems is $LiNbO_3$, which can be quasi-phasematched using a combination of lithographic patterning and electric field poling to produce domains of alternating polarity [2]. However, multiphonon absorption in lithium niobate makes efficient operation difficult for wavelengths longer than 4 μm, especially at high average powers.

For NLO generation of IR and THz wavelengths, GaAs is a promising material due to its large nonlinear susceptibility ($d_{14} = 94$ pm/V), broad transparency range in the IR (0.9–18 μm), high thermal conductivity (46 W/m K), and mature processing technologies. Unlike lithium niobate, GaAs is not ferroelectric, so a different scheme must be implemented to produce the patterned structures for QPM. Periodic inversion has been achieved using stacks of GaAs plates with alternating orientation in configurations where the plates were discrete [3,4], bonded [5,6], or bonded and epitaxially regrown [7]; however, it is challenging to maintain periodicity in the stack and to access short periods. An alternative approach to creating patterned structures requires first producing a layer of inverted (antiphase) GaAs on a GaAs substrate. The inverted layer can either be fabricated by wafer bonding [8–10] or through an all-epitaxial GaAs/Ge/GaAs approach that uses a nonpolar Ge layer to reverse the GaAs orientation [11–13]. Using lithography and selective chemical etching, alternating regions of the inverted layer and substrate are exposed, producing a template with a periodic crystallographic inversion. Thick regrowth on the template produces a grating. The templates and thick layers are known as orientation-patterned GaAs (OP-GaAs). To provide a sufficient aperture for the laser beams during NLO frequency conversion, the OP-GaAs thickness typically must exceed 500 μm for IR devices and 1 mm for THz devices. These specifications pose a unique challenge—very thick epitaxial growth of a patterned structure.

OP-GaAs gratings are being used to generate IR and THz radiation. A tunable THz source based on intracavity parametric down-conversion has been developed [14]. Recent results have demonstrated 0.5 mW at 1.3 THz using an 800-μm-thick OP-GaAs layer [15]. By optical parametric oscillation (OPO) in an OP-GaAs sample with a 60.5 μm grating period, 647 mW of mid-IR average output power (signal plus idler) was produced at 25% overall efficiency (30% slope) [16]. Also, an OP-GaAs OPO has been used to generate tunable 2–11 μm wavelength pulses [17] and has been successfully pumped with circularly polarized and depolarized light [18]. A 4.5–10.7 μm broadband mid-IR continuum was produced by optical parametric generation in OP-GaAs [19].

* Corresponding author. Tel.: +1 781 377 7111; fax: +1 781 377 6948.
E-mail address: candace.lynch@hanscom.af.mil (C. Lynch).

0022-0248/$ - see front matter Published by Elsevier B.V.
doi:10.1016/j.jcrysgro.2008.08.050

REPORT DOCUMENTATION PAGE

Form Approved
OMB No. 0704-0188

1. REPORT DATE *(DD-MM-YYYY)*	2. REPORT TYPE	3. DATES COVERED *(From - To)*
08-01-2009	Journal Article	14 Feb 08 – 05 Aug 08

4. TITLE AND SUBTITLE

Growth of mm-thick orientation-patterned GaAs for IR and THZ generation

5a. CONTRACT NUMBER
In-House

5b. GRANT NUMBER

5c. PROGRAM ELEMENT NUMBER
62204F

6. AUTHOR(S)

*C. Lynch, D. Bliss, T. Zens, **A. Lin, J. S. Harris, ***P. S. Kuo and M. M. Fejer

5d. PROJECT NUMBER
4916

5e. TASK NUMBER
HC

5f. WORK UNIT NUMBER
01

7. PERFORMING ORGANIZATION NAME(S) AND ADDRESS(ES)

*AFRL/RYHC, 80 Scott Drive, Hanscom AFB, MA 01731; **Solid State Photonics Laboratory, Standford University, Stanford, CA 94305; ***E. L. Ginzton Laboratory, Stanford University, Stanford, CA 94305

8. PERFORMING ORGANIZATION REPORT

9. SPONSORING / MONITORING AGENCY NAME(S) AND ADDRESS(ES)

Electromagnetics Technology Division Source Code: 437890
Sensors Directorate
Air Force Research Laboratory
80 Scott Drive
Hanscom AFB MA 01731-2909

10. SPONSOR/MONITOR'S ACRONYM(S)

11. SPONSOR/MONITOR'S REPORT NUMBER(S)
AFRL-RY-HS-TP-2009-0001

12. DISTRIBUTION / AVAILABILITY STATEMENT

Distribution A: Approved for public release; distribution unlimited.

13. SUPPLEMENTARY NOTES

The U. S. Government is joint author of this work and has the right to use, modify, reproduce, release, perform, display, or disclose the work. Published in Journal of Crystal Growth, 310 (2008) 5241-5247. Cleared for Public Release by ESC/PA number: ESC-08-0188

14. ABSTRACT

Infrared and terahertz frequency generation by compact and rugged laser optical systems is of interest for both commercial and military applications. Lasers emitting in the IR and THz can be produced using nonlinear frequency conversion from shorter wavelength pump laser sources. This paper describes the process of crystal growth for production of quasi-phase matched structures in GaAs for nonlinear frequency conversion. The method described is low-pressure hydride vapor phase epitaxy for regrowth of thick GaAs on orientation-patterned templates. Very high growth rates are achieved to produce grating patterns of 1 millimeter thickness, with nearly vertical walls. The process improvements needed for successful crystal growth are discussed.

15. SUBJECT TERMS

Hydride vapor phase epitaxy, Gallium arsenide, Nonlinear optic materials

16. SECURITY CLASSIFICATION OF:			17.LIMITATION OF ABSTRACT	18.NUMBER OF PAGES	19a. NAME OF RESPONSIBLE PERSON
a. REPORT	b. ABSTRACT	c.THIS PAGE			Candace Lynch
Unclassified	Unclassified	Unclassified	SAR	7	19b. TELEPHONE NUMBER *(include area code)* n/a

Standard Form 298 (Rev. 8-98)
Prescribed by ANSI Std. Z39.18

In what follows, we discuss the growth of mm-thick OP-GaAs on patterned templates, building on prior efforts that demonstrated 650-μm-thick gratings [20]. Since the thicknesses necessary for OP-GaAs are not practically attainable using molecular beam epitaxy (MBE) or organo-metallic vapor phase epitaxy (OMVPE), we used low-pressure hydride vapor phase epitaxy (HVPE), which can have much higher growth rates [21]. To produce mm-thick layers, it is desirable to establish a rate of at least 100 μm/h and maintain that rate for approximately 10 h. Due to the tendency for parasitic deposition of GaAs on the quartz reactor walls, the total length of productive growth time may be limited as the vapor becomes depleted. Growth of OP-GaAs requires vertical propagation of the grating through the HVPE layer. Unfortunately, the domain walls tend to deviate from the initial pattered structure, reducing the efficiency of the nonlinear interaction. We will discuss the interplay between the growth conditions, template design, substrate wafer orientation, surface morphology, and the quality of the domain wall propagation. These discoveries have led to the production of mm-thick films with domain widths of 20 μm—an aspect ratio of 50:1.

2. Epitaxial growth and characterization

HVPE was performed in a custom-built reactor at the AFRL Hanscom Research Site [20]. A schematic of the reactor is shown in Fig. 1; it consists of a horizontal, three-zone, resistively heated furnace, and a pump to allow operation at low pressure (approximately 5 Torr). Gallium was transported as GaCl by reacting HCl with liquid gallium held in a quartz boat. Undiluted AsH_3 was used as the arsenic source, with a nominal III/V ratio of 0.5. A secondary HCl supply provided a means to control the supersaturation. Typical gas flows are listed in Table 1; the total flow was approximately 200–300 sccm at a velocity of 24 cm/s. Temperatures in the ranges of 720–730 °C (Ga source zone), 730–770 °C (mixing zone), and 690–720 °C (deposition zone) have been investigated. All of the results presented in this work were obtained using growth conditions within the ranges given above and in Table 1. Wafers were held in the deposition zone using a custom-made quartz sled. The design of the sled allowed one or two substrates (usually $\frac{1}{4}$ of a 2 in diameter wafer) to be fixed in a nearly vertical orientation with quartz baffles in front of and behind the wafers. During some of the HVPE runs, interruptions in the film growth were used to create witness marks—these lines identify the thickness and surface morphology progression during the long growths.

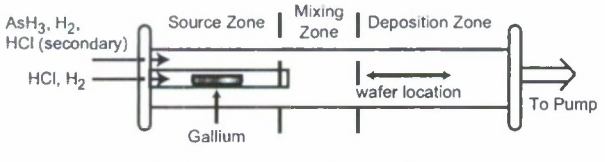

Fig. 1. Schematic of GaAs HVPE reactor.

Table 1
Mass flow rates used in this study

Gas	Flow (sccm)
AsH_3	70
HCl (over Ga)	35
HCl (secondary)	0–45
H_2 (over Ga)	28
H_2 (carrier)	65–110

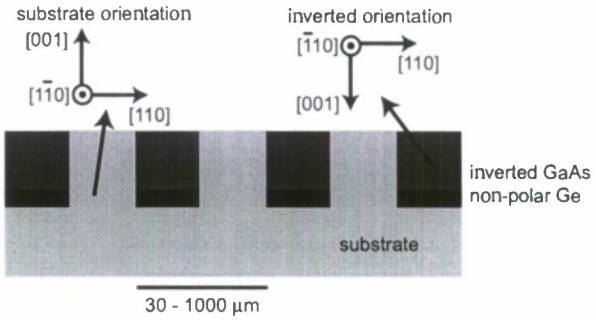

Fig. 2. Crystallographic relationship between the two orientations. In this schematic, the substrate misorientation of 4° toward (1 1 1)B is not depicted.

Thick GaAs layers were grown on as-received semi-insulating GaAs wafers, and on OP-GaAs templates produced at Stanford University. The fabrication of these templates is described in Ref. [11]; a brief overview is given here. MBE was used to grow a GaAs/Ge/GaAs heterostructure. Under the appropriate MBE conditions, the GaAs grown on the Ge is crystallographically inverted with respect to the GaAs substrate. After lithographically defining the grating pattern, chemical etching was used to selectively expose the substrate through the MBE GaAs/Ge layers to form a template grating. These gratings consist of alternating domains of the substrate and inverted orientation—a schematic indicating the crystallographic relationship between the domains is shown in Fig. 2. Due to the symmetry of the GaAs zincblende structure, the orientation of the inverted domains is equivalent to a 90° rotation about [0 0 1]. In most of the templates used, multiple gratings (each with a different periodicity) were surrounded by unpatterned regions ("streets"). A requirement for the successful growth of inverted GaAs on Ge during the MBE process is the use of slightly misoriented substrates. This misorientation facilitates the annihilation of antiphase domains during the MBE growth of GaAs on Ge. All of the OP-GaAs templates and the as-received substrates in this study had a misorientation of 4° toward (1 1 1)B.

Samples were studied post-growth by cross-sectional Nomarski contrast microscopy, scanning electron microscopy (SEM), and atomic force microscopy (AFM). Surface roughness measurements were made using 40 μm × 40 μm AFM scans. In thinner films (<300 μm), cross-sections were obtained by cleaving and etching in a $NH_4OH/H_2O_2/H_2O$ solution. Thick gratings were separated using a diamond saw, polished using alumina powder, followed by chemomechanical polishing and the same etch as above.

3. High growth rates and thick layer production

High growth rates have been attributed to the near-equilibrium nature of HVPE [22]. This is unlike MBE and OMVPE growth, where the growth occurs in a regime far from equilibrium, and the growth rates are typically on the order of a few microns per hour. By controlling the supersaturation in the gas phase during atmospheric pressure HVPE, a wide range of etch and growth rates are attainable. Enhanced growth rates during low-pressure HVPE were reported by Gruter, who postulated that reduced operating pressures enhance the growth rate of GaAs by hindering the cracking of arsine [21]. In this case, the dominant growth reaction switches from:

$$GaCl + \tfrac{1}{2}H_2 + \tfrac{1}{4}As_4 \overset{K_1}{\longleftrightarrow} GaAs + HCl \quad (1)$$

to

$$GaCl + AsH_3 \xleftrightarrow{K_2} GaAs + HCl + H_2 \quad (2)$$

The latter reaction is significantly more thermodynamically favorable (K_1~5; K_2~4×10^4) and produces a much greater supersaturation, leading to a higher growth rate.

We evaluated the growth rates by conducting 1-h-long depositions on unpatterned GaAs wafers with the standard 4° miscut. Average growth rates ranging ~50–200 μm/h have been observed, and are controllable by varying the growth temperature. Shaw [23] was the first to systematically study the dependence of growth rate on temperature, and characterized two regimes of growth behavior during VPE—surface kinetics-limited at low temperatures and mass transfer-limited at high temperatures. At low temperatures, the rate-limiting process(es), such as adsorption [24] or chlorine desorption [25], are thermally activated, and the growth rate increases with increasing temperature. The behavior in the second regime results from the temperature dependence of the thermodynamic driving force and the growth rate decreases with increasing temperature. The interplay between the two regimes produces a maximum in the growth rate. A series of 1-h-long depositions on bare wafers demonstrated this behavior (Fig. 3); the temperature was varied by changing the location of the wafer holder within the furnace. The wafer positions represented in Fig. 3 span less than 1.5 cm and the gas composition is assumed to be uniform across this range. Since the wafer is held vertically, we do not expect the horizontal furnace temperature gradient to affect uniformity across the wafer surface. However, there is a radial thickness variation across the wafer—with thicker growth at the edges. We have correlated this variation with the position of the baffle in front of the wafer. At small baffle-wafer spacing, the thickness variation is significant; increasing the spacing results in a reduction in the thickness variation. To compare growth rates between wafers, we cleave samples from the as-grown wafers at the same relative locations each time. Multiple thickness measurements are taken from each cleaved cross-section and are averaged. For the data presented in Fig. 3, the thickness variation along each cross-section was not more than 3%.

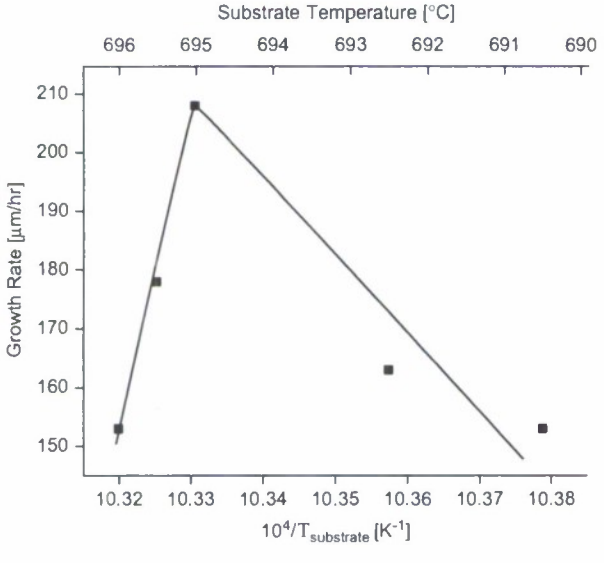

Fig. 3. Average growth rates for 1-h-long runs on bare (001) GaAs substrates with a 4°→(111)B miscut.

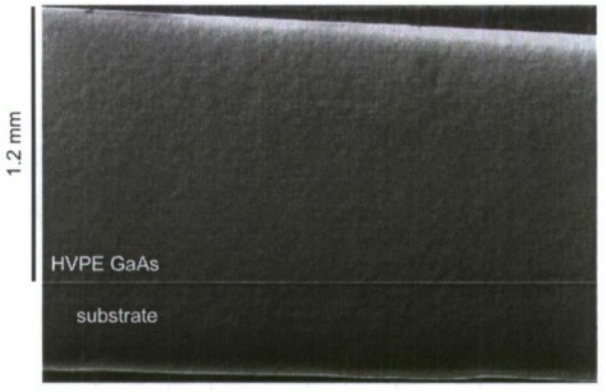

Fig. 4. Polished and etched cross-section of mm-thick HVPE GaAs following 10 h of deposition on a bare (001) GaAs substrate with a 4°→(111)B miscut.

The narrow temperature range for fast growth shown in Fig. 3 is unlike the broad peak seen in our earlier work [20]. Although the current growth conditions (chemistry and temperature profile) have been altered to optimize the growth rate and material quality, they are not drastically different from those in our prior work. Instead, we suggest that the narrow peak shown in Fig. 3 results from modifications to the reactor hardware, specifically, the positioning of baffles at the reactor inlet, in front of, and behind the wafer(s). These baffles alter the gas flow, improve mixing, and may also affect the thermal profile.

Increasing the duration of growth runs typically results in a decline in growth rate with respect to time due to parasitic GaAs deposition on the quartz reactor walls and on the wafer carrier. Initially, GaAs nucleates on the colder quartz downstream of the sample; with time, the coated region spreads forward and eventually includes the quartz in front of the sample. This deposition depletes the vapor, reducing the growth rate on the wafer surface. To mitigate this problem, we introduced a thermal profile that dropped sharply at the substrate, which suppressed upstream deposits. Such a profile can be created by adjustment of the mixing zone and deposition zone temperatures and by placement of quartz baffles to establish a separate central hot mixing zone. While increasing the mixing zone temperature results in less parasitic growth, it also impacts the magnitude of unintentional silicon doping and the free carrier concentration. Since low free carrier concentrations are desired to minimize optical absorption, the mixing zone temperature must be chosen to balance both considerations. We also find that a secondary HCl flow is beneficial for retarding the parasitic growth by providing a reduction in supersaturation [26].

Although our early efforts required the use of multiple growth steps [27], we have now demonstrated over 1 mm of GaAs deposition in a single run. Fig. 4 is an optical micrograph of a polished and etched cross-section representing 10 h of growth. The total thickness is 1.2 mm—an average growth rate of 120 μm/h.

4. Thick growth on OP-GaAs templates

To produce NLO devices, HVPE regrowth is conducted on OP-GaAs template wafers patterned with gratings of alternating GaAs orientation. These structures are periodic antiphase (inversion) domains with widths ranging 20 μm–2 mm, depending on the coherence length needed for the final application. In the HVPE layer, it is necessary for the domain walls to remain orthogonal to the substrate, so that the domain widths are maintained constant throughout the film thickness.

For OP-GaAs, the desired antiphase domain wall orientation is along {1 1 0} planes, and consists of alternating Ga–Ga and As–As bonds along the [0 0 1] direction. {1 1 0} antiphase boundaries (APBs) in GaAs have the lowest formation energy per unit area [28], and transmission electron microscopy (TEM) investigations have found the {1 1 0} orientation to be the most common [29]. This suggests that OP-GaAs layers with periodic {1 1 0} APBs should be attainable. However, we have found a tendency for the domain walls to deviate from vertical, leading to tapering of one set of domains, and potentially resulting in single-phase material at the top of the layer (Fig. 5). We have identified and addressed several mechanisms for this annihilation, leading to the production of mm-thick layers with nearly vertical domain walls.

The quality of thick orientation-patterned growth depends on the design of the initial template. The template must be aligned to allow the laser beams taking part in frequency conversion to propagate across the grating in one of the in-plane ⟨1 1 0⟩ directions. The substrate misorientation imposes an additional constraint on the template alignment: when fabricating OP-GaAs templates on substrates misoriented toward (1 1 1)B, the {1 1 0} domain walls can be aligned either parallel to or perpendicular to the miscut. Specifically, domain walls on $(1\bar{1}0)$ planes are perpendicular to the miscut; walls on (1 1 0) planes are parallel to the miscut. A schematic depicting the relationship between these two alignments is shown in Fig. 6. For illustrative purposes, two gratings are drawn above the surface; in actuality the top of the gratings is at approximately the same height as the rest of the epitaxial layer. Both alignments have been used; however, OP-GaAs growth is problematic when the domain walls are initially aligned perpendicular to the miscut [20] (Fig. 7). During such growth, vertical domain walls are not formed, because the $(1\bar{1}0)$ planes are tilted with respect to the substrate normal. Additionally, there is a tendency for a subset of the walls to bend sharply, resulting in loss of the original periodic pattern. Therefore, when miscut substrates are used in the fabrication of OP-GaAs templates, the misorientation must be aligned along the domain walls.

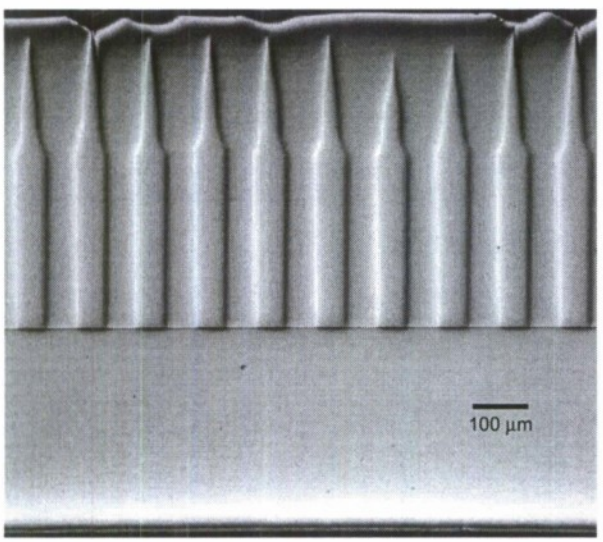

Fig. 5. Cleaved and etched $(1\bar{1}0)$ cross-section of a 550-μm-thick OP-GaAs layer following 8 h of deposition. The grating structure is eliminated at the top of the layer due to annihilation of the antiphase domains.

Another significant effect of the substrate misorientation is the establishment of a step-flow growth mode. Under typical HVPE growth conditions, the deposition rate is dependent on the magnitude of the misorientation [20]. This property is indicative of step-flow growth, because the density of steps scales with the angle of miscut. In a step-flow regime, adatoms migrating on surface terraces attach to the steps, which translate across the surface, increasing the film thickness. Although step-flow behavior is beneficial for achieving fast growth rates, it introduces problems for growth on patterned substrates. Steps propagating across a street are pinned as they encounter a grating, resulting in step bunching at the interfaces between the unpatterned streets and the gratings. This leads to the formation of macroscopically large steps—for example, the SEM images in Fig. 8 show streets which are approximately 200 μm higher than the adjacent gratings. During thick growth, the region at the bottom of the step facets toward (0 0 1), producing significant thickness variations along the grating in the direction of the substrate misorientation. The surface of the grating in Fig. 8b has tilted approximately 4° away from the substrate/film interface, accommodating the initial miscut with a macrostep and a large (0 0 1) terrace.

In addition to the presence of step bunching, the most notable feature in Fig. 8a is overgrowth of the street onto the gratings. This overgrowth progresses in the direction of step-flow, and can completely destroy a grating within a few hundred microns of growth. The street overgrowth can be mitigated by using templates without streets; however, this is often undesirable because it limits the ability to produce a variety of grating dimensions on one wafer. Alternatively, templates can be designed such that the streets also have the inverted orientation.

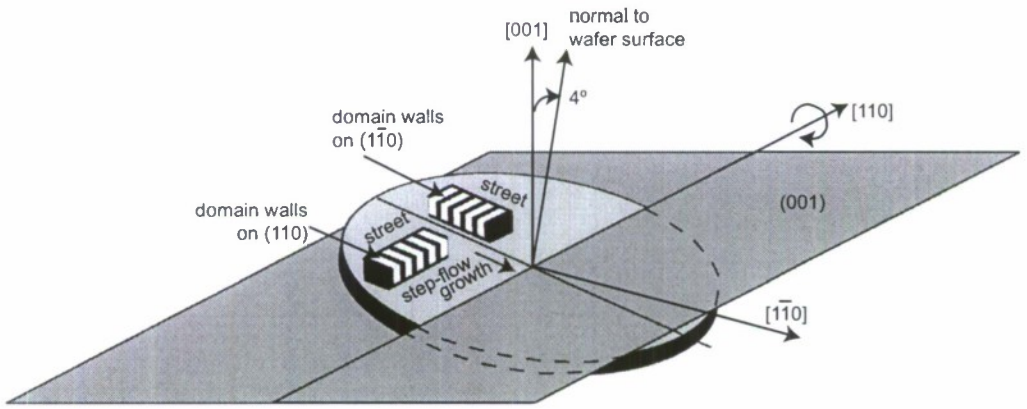

Fig. 6. Schematic relationship between the substrate misorientation and two possible grating alignments.

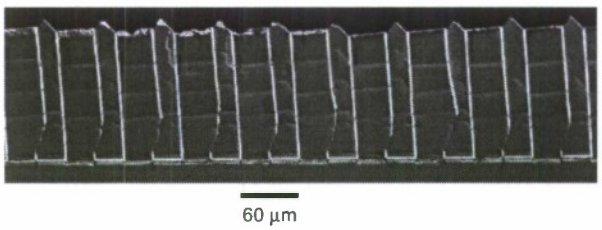

Fig. 7. (110) Cross-section of HVPE growth on a template with the grating walls aligned perpendicular to the substrate tilt (i.e., on (1 $\bar{1}$ 0)). The faint horizontal bands result from growth interruptions used to reveal the intermediate surface structure.

These templates are less prone to street overgrowth during the HVPE regrowth (Fig. 8b). On templates with inverted polarity streets, step bunching at the street/grating interface produces a {113}A facet with little to no evidence of overgrowth.

During thick HVPE growth on OP-GaAs templates, the surface evolves to form low index facets along the individual domains. The growth conditions in Table 1 typically result in the formation of {111}B facets along the inverted domains (see Fig. 9). Faceting of the alternate set of domains (i.e., those with the orientation of the substrate) is occasionally observed in regions where street overgrowth is occurring, and presents {113}A surfaces. The domains with the same orientation as the substrate have {*hkl*}A facets due to the alignment of the domain walls with the 4°→ (111)B tilt; the inverted domains have {*hkl*}B facets since the inversion is equivalent to a 90° rotation. Faceting of the individual domains results from the strong dependence of growth rate on crystallographic orientation. Studies conducted during atmospheric pressure VPE have shown that temperature and gas composition affect the relative growth rates of the different orientations [23]. Selective growth by atmospheric pressure HVPE on GaAs mesas demonstrated that the appearance of {001}, {110}, and {111} faces varied with the III/V ratio, supersaturation, and temperature [30]. We have investigated facet formation over a range of gas chemistries and growth temperatures during low-pressure HVPE and have only observed {111}B facets on inverted GaAs, {113}A facets on substrate-oriented GaAs, and (001) vicinal surfaces.

Control over the faceting behavior is desired because the onset of faceting can lead to destabilization of the vertical wall propagation. The faceted domains slowly overtake the adjacent domains, leading to a slow loss of the 50–50 grating duty cycle, and eventual annihilation of the antiphase domains. For example, many of the domain walls in Fig. 9 are not perfectly vertical; the walls bounding {111}B facets tilt outwards. This tilting may result from the lateral component of the {111}B facet growth direction. In the narrow domains used for IR generation, complete annihilation can happen in layers thinner than 500 μm, whereas the wide gratings for THz are relatively unaffected. Using cross-sectional micrographs, we measured the deviation from (110) of the walls separating the domains. The tilting is usually evident within the first 20 μm of growth, and in most cases the angle remains constant through the entire layer thickness. The angles exhibited by individual walls range 0.2–1.1°. Both walls bounding the inverted domains tilt outward, leading to a net spread of 0.7–1.9° per domain. In Fig. 10 (left axis), this angle is plotted as a function of growth temperature for a series of 1-h growths conducted with identical gas flows. Higher temperatures lead to greater deviations from (110); lower growth temperatures are therefore preferred to minimize the effect of wall tilting and domain annihilation. Although a variation in the growth temperature also affects the growth rate, we did not observe any correlation between the wall tilting angles and the growth rate.

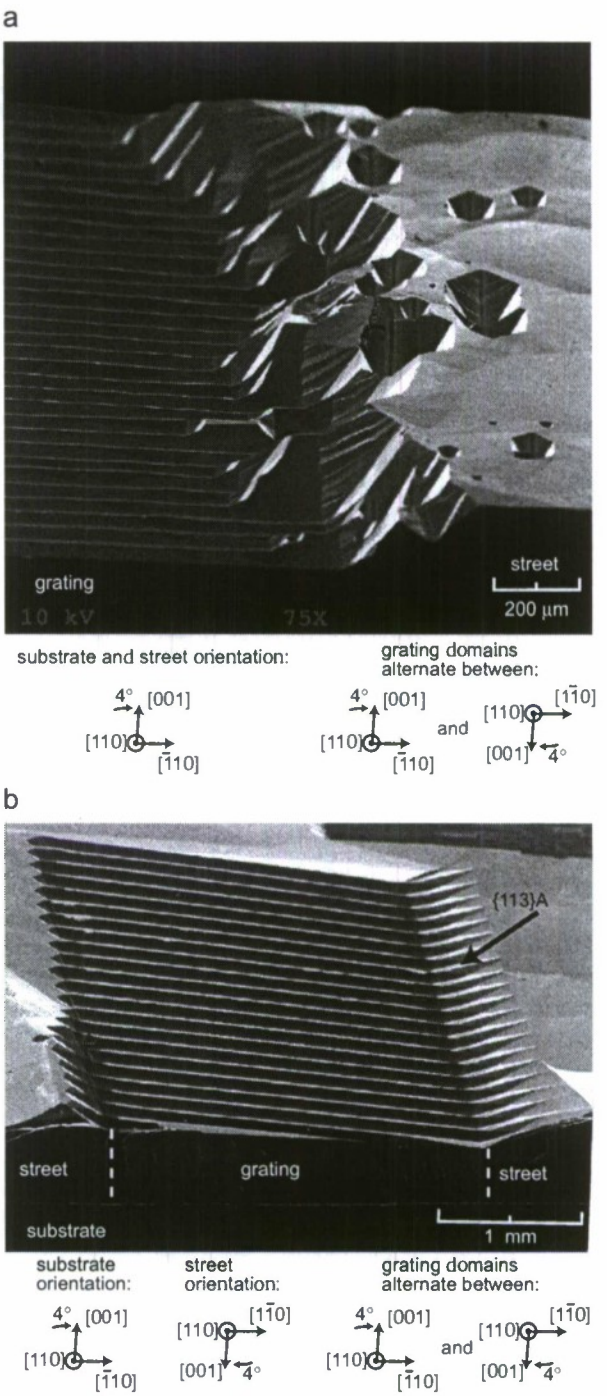

Fig. 8. SEM images of the OP-GaAs surface following HVPE growth. (a) Growth on a template with the street polarity the same as the substrate. The grating is on the left side, an unpatterned street is on the right, and a 200 μm-high step separates the two. The average growth rate was approximately 79 μm/h. (b) Growth on a template with inverted polarity streets. The average growth rate was approximately 95 μm/h.

A comparison of this data with AFM measurements of the surface roughness of bare (unpatterned) GaAs wafers grown in

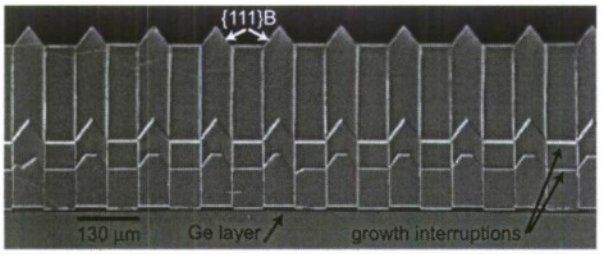

Fig. 9. (1 $\bar{1}$ 0) Cross-section of HVPE growth on a template with the grating walls aligned parallel to the substrate tilt. The horizontal bands result from growth interruptions used to reveal the intermediate surface structure.

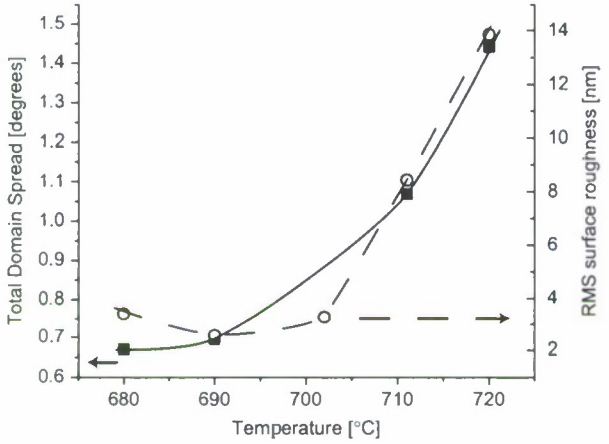

Fig. 10. *Solid line*: average domain wall tilting (represented as the sum of the average tilts of walls to the left and right of a Ge layer) for gratings grown at substrate temperatures between 680 and 720 °C. *Dashed line*: RMS surface roughness measured after growth on as-received (unpatterned) wafers.

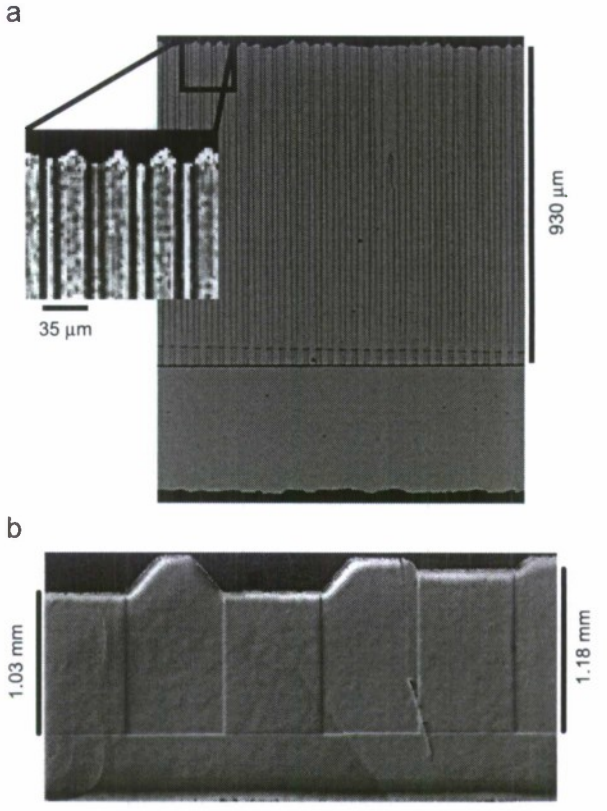

Fig. 11. (1 $\bar{1}$ 0) Cross-sections of approximately 1-mm-thick OP-GaAs layers with near-vertical domain walls. (a) Represents a grating appropriate for IR generation (18.5 μm domain width), the grating in (b) is intended for THz generation (700 μm domain width).

tandem with the OP-GaAs gratings indicates that the domain wall spreading increases as the surface roughness increases (Fig. 10, right axis). The rough surfaces consist of [1 1 0]-oriented ripples that are 10–50 nm in height and 15–30 μm wide. The origin of these ripples may be related to step bunching and faceting of the surface. This observation reinforces the need for lower growth temperatures during production of OP-GaAs gratings.

The appropriate selection of growth conditions and template design has led to the production of mm-thick OP-GaAs with near-vertical walls, suitable for use in IR (Fig. 11a) and THz (Fig. 11b) generation. The gratings shown in Fig. 11 were grown on templates with inverted polarity streets; growth conditions were within the ranges given in Section 2. Total HVPE growth times were 10 and 11 h for the OP-GaAs in Fig. 11a and b, respectively, representing average growth rates of 93 and 94 μm/h. High aspect ratios were achieved using templates with narrow domains, for example, the domains in Fig. 11a were initially 18.5 μm wide and propagate through the entire 930 μm film, representing an aspect ratio of 50:1.

5. Summary

Thick orientation-patterned GaAs films, desirable for generation of IR and THz frequencies by NLO frequency conversion, have been obtained. Establishing and maintaining the high growth rates necessary for mm-thick epitaxial growth has been successfully demonstrated using HVPE at low pressures. Growth rates up to 200 μm/h and total thicknesses over 1 mm were attained by controlling the reactor temperature profile and vapor supersaturation. Orientation-patterned GaAs gratings, which have periodic reversals in the crystallographic orientation, allow efficient NLO conversion through QPM. The challenge for growth of these structures arises from the tendency for the domains to annihilate and form a layer of uniform orientation. We have found that choices in the template design have an important impact on the success of the HVPE regrowth. The domain walls must be aligned with the substrate miscut of 4° toward (1 1 1)B, and any unpatterned regions should have the inverted orientation relative to the substrate. Lower growth temperatures result in a lesser degree of domain wall tilting, which is beneficial for achieving thick layers without variation in the domain widths. We have produced mm-thick OP-GaAs with domain walls that extend through the thickness of the layer. These structures are suitable for IR and THz generation and efforts are underway to characterize their device performance.

Acknowledgments

The authors would like to thank Marta Garcia and Michael Suscavage for the SEM images. Xiaojun Yu was responsible for some of the template fabrication.

References

[1] D.S. Hum, M.M. Fejer, C.R. Phys. B (2007) 180.
[2] L.E. Myers, R.C. Eckardt, M.M. Fejer, R.L. Byer, W.R. Bosenberg, J.W. Pierce, J. Opt. Soc. Am. B 12 (1995) 2102.
[3] A. Szilagyi, A. Hordvik, H. Schlossberg, J. Appl. Phys. 47 (1976) 2025.
[4] D.E. Thompson, J.D. McMullen, D.B. Anderson, Appl. Phys. Lett. 29 (1976) 113.
[5] L.A. Gordon, G.L. Woods, R.C. Eckardt, R.K. Route, R.S. Feigelson, M.M. Fejer, R.L. Byer, Electron. Lett. 29 (1993) 1942.
[6] E. Lallier, L. Becouarn, M. Brevignon, J. Lehoux, Electron. Lett. 34 (1998) 1609.
[7] L. Becouarn, B. Gerard, M. Brevingnon, J. Lehoux, Y. Gourdel, E. Lallier, Electron. Lett. 34 (1998) 2409.
[8] S.J.B. Yoo, R. Bhat, C. Caneau, M.A. Koza, Appl. Phys. Lett. 66 (1995) 3410.
[9] D. Faye, E. Lallier, A. Grisard, B. Gerard, E. Gil-Lafon, Mater. Res. Soc. Symp. Proc. 799 (2003) 79.
[10] Jin Li, David B. Fenner, Krongtip Termkoa, Mark G. Allen, Peter F. Moulton, Candace Lynch, David F. Bliss, William D. Goodhue, Proc. SPIE 6875 (2008) 687SOH.
[11] C.B. Ebert, L.A. Eyres, M.M. Fejer, J.S. Harris, J. Crystal Growth 201/202 (1999) 187.
[12] L.A. Eyres, P.J. Tourreau, T.J. Pinguet, C.B. Ebert, J.S. Harris, M.M. Fejer, L. Becouarn, B. Gerard, E. Lallier, Appl. Phys. Lett. 79 (2001) 904.
[13] Shinji Koh, Takashi Kondo, Minoru Ebihara, Tetsuya Ishiwada, Hidetaka Sawada, Hideki Ichinose, Ichiro Shoji, Ryoichi Ito, Jpn. J. Appl. Phys. 38 (1999) L508.
[14] J.E. Schaar, K.L. Vodopyanov, P.S. Kuo, M.M. Fejer, X. Yu, A. Lin, J.S. Harris, D. Bliss, C. Lynch, V.G. Kozlov, W. Hurlbut, IEEE J. Sel. Top. Quantum Electron. 14 (2008) 354.
[15] K. Vodoyopanov, J.E. Schaar, M.M. Fejer, unpublished results.
[16] Peter G. Schunemann, In: Proceedings of SPIE—The International Society for Optical Engineering 6455, Nonlinear Frequency Generation and Conversion: Materials, Devices, and Applications VI, 2007, 64SS0R.
[17] K.L. Vodopyanov, O. Levi, P.S. Kuo, T.J. Pinguet, J.S. Harris, M.M. Fejer, B. Gerard, L. Becouarn, E. Lallier, Opt. Lett. 29 (2003) 1912;
K.L. Vodopyanov, O. Levi, P.S. Kuo, T.J. Pinguet, J.S. Harris, M.M. Fejer, B. Gerard, L. Becouarn, E. Lallier, Proc. SPIE 5620 (2004) 63.
[18] P.S. Kuo, K.L. Vodopyanov, M.M. Fejer, X. Yu, J.S. Harris, D.F. Bliss, D. Weyburne, Opt. Lett. 32 (2007) 2735.
[19] P.S. Kuo, K.L. Vodopyanov, M.M. Fejer, D.M. Simanovskii, X. Yu, J.S. Harris, D. Bliss, D. Weyburne, Opt. Lett. 31 (2006) 71.
[20] D.F. Bliss, C. Lynch, D. Weyburne, K. O'Hearn, J.S. Bailey, J. Crystal Growth 287 (2006) 673.
[21] K. Gruter, M. Deschler, H. Jurgensen, R. Beccard, P. Balk, J. Crystal Growth 94 (1989) 607.
[22] S. Lourdudoss, O. Kjebon, IEEE J. Sel. Top. Quantum Electron. 3 (1997) 749.
[23] D. Shaw, J. Crystal Growth 31 (1975) 130.
[24] D.W. Shaw, J. Electrochem. Soc. 117 (1970) 683.
[25] R. Cadoret, E. Gil-Lafon, J. Phys. I France 7 (1997) 889.
[26] T. Mizutani, H. Watanabe, J. Crystal Growth 59 (1982) 507.
[27] C. Lynch, D. Bliss, T. Zens, D. Weyburne, J. Jimenez, M. Avella, P.S. Kuo, X. Yu, IEEE Proceedings on Indium Phosphide and Related Materials, 2006, p. 151.
[28] D. Vanderbilt, C. Lee, Phys. Rev. B 45 (1992) 192.
[29] N.-H. Cho, B.C. De Cooman, C.B. Carter, R. Fletcher, D.K. Wagner, Appl. Phys. Lett. 47 (1985) 879.
[30] E. Gil-Lafon, J. Napierala, D. Castelluci, A. Pimpinelli, R. Cadoret, B. Gerard, J. Crystal Growth 222 (2001) 482.